ECCENTRIC MERGERS OF BLACK HOLES WITH SPINNING NEUTRON STARS

William E. East[1], Vasileios Paschalidis[2], and Frans Pretorius[2]

[1]Kavli Institute for Particle Astrophysics and Cosmology, Stanford University, SLAC National Accelerator Laboratory, Menlo Park, CA 94025, USA
[2]Department of Physics, Princeton University, Princeton, NJ 08544, USA
Draft version June 29, 2015

ABSTRACT

We study dynamical capture binary black hole–neutron star (BH–NS) mergers focusing on the effects of the neutron star spin. These events may arise in dense stellar regions, such as globular clusters, where the majority of neutron stars are expected to be rapidly rotating. We initialize the BH–NS systems with positions and velocities corresponding to marginally unbound Newtonian orbits, and evolve them using general-relativistic hydrodynamical simulations. We find that even moderate spins can significantly increase the amount of mass in unbound material. In some of the more extreme cases, there can be up to a third of a solar mass in unbound matter. Similarly, large amounts of tidally stripped material can remain bound and eventually accrete onto the BH—as much as a tenth of a solar mass in some cases. These simulations demonstrate that it is important to treat neutron star spin in order to make reliable predictions of the gravitational wave and electromagnetic transient signals accompanying these sources.

Subject headings: black hole physics—gamma-ray burst: general—gravitation—gravitational waves—stars: neutron

1. INTRODUCTION

Next generation ground-based gravitational wave (GW) detectors such as aLIGO (Abramovici et al. 1992) are expected to reach design sensitivity within the next few years. Among their most promising sources are mergers of compact objects (COs), including black hole–neutron star (BH–NS) binaries. BH–NS mergers are also proposed short-hard gamma-ray burst (sGRB) engines (e.g. Meszaros (2006)), and may power other electromagnetic (EM) transients either preceding (Hansen & Lyutikov 2001; McWilliams & Levin 2011; Paschalidis et al. 2013) or following (Metzger & Berger 2012) the merger. These EM counterparts to GWs could be observed by current and future wide-field telescopes such as PTF (Rau 2009) and LSST (LSST Dark Energy Science Collaboration 2012).

Extracting maximum information from such "multi-messenger" observations requires careful modeling of BH–NS mergers. Several studies of quasicircular BH–NS inspirals using numerical relativity simulations have been performed, see, e.g., Chawla et al. (2010); Etienne et al. (2012); Kyutoku et al. (2013); Tanaka et al. (2014); Foucart et al. (2014). While quasicircular binaries may dominate the global rates of BH–NS encounters in the Universe, recent calculations (Kocsis & Levin 2012; Lee et al. 2010; Samsing et al. 2014) suggest that in dense stellar regions, such as galactic nuclei and globular clusters (GCs), CO binaries can form through dynamical capture and merge with non-negligible eccentricities. Compared to quasi-circular inspirals, these emit more GW energy in the high luminosity, strong-field regime of general relativity, and small changes in the energy of the binary at each pericenter passage can lead to relatively large changes in the time between GW bursts—the leading order GW observable. Hence these systems could be excellent laboratories to test gravity and measure the internal structure of a NS (insofar as this affects the energy of the orbit, e.g. tidal excitation of f-modes). Rates of these events are highly uncertain, but have been estimated to be up to ~ 100 yr^{-1} Gpc^{-3}. To realize this rich potential to learn about the Universe from eccentric mergers, it is irrelevant what their rates are compared to quasi-circular inspiral, only that eccentric mergers occur frequently enough that some events could be observable by aLIGO within its lifetime. However, new detection pipelines would be needed that are better adapted to the repeated-burst nature of eccentric GW mergers for aLIGO to efficiently detect them (Tai et al. 2014). For more discussion of rates, distinguishing features, and detection issues for eccentric encounters, see East et al. (2013) and references therein.

Motivated by the above, Stephens et al. (2011); East et al. (2012a) performed fully general-relativistic hydrodynamical (GR-HD) simulations of dynamical-capture BH–NS mergers. These studies explored the effects of impact parameter, BH spin, and NS equation of state (EOS) on GW emission and post-merger BH disk and ejecta masses. Here, we expand upon this work by including the effects of NS spin. To date the only simulations including spinning NSs focused on quasicircular NS–NS mergers, e.g. Tichy (2011); Bernuzzi et al. (2014), demonstrating that even moderate spins can affect the dynamics.

NS spin has two main effects: (1) it modifies the star's structure, making it less gravitationally bound; (2) it changes the orbital dynamics, e.g., by shifting the effective innermost stable orbit (ISO). This can impact not only the GWs from CO mergers, but also the amount of matter forming the BH accretion disk that putatively powers a sGRB, and the amount of unbound matter that powers other EM transients, such as kilonovae. There may also be effects on pre-merger EM signals since the NS spin determines the light-cylinder radius, and hence

the orbital separation at which unipolar induction turns on.

Spin effects on the NS structure cannot be neglected if the NS spin period P is $\mathcal{O}(\mathrm{ms})$. Furthermore, for comparable mass BH–NSs near the tidal disruption radius, NS spin effects on the orbit will be non-negligible when P is similar to the BH–NS encounter timescale (Tichy 2011). For example, a BH–NS eccentric encounter with mass ratio $q = M_{BH}/M_{NS} = 4$ (as studied here) near a periapse of $r_p = 10M$ has an interaction timescale of $t_{int} \simeq (r_p^3/M)^{1/2} \sim 1.0(M_{NS}/1.4M_\odot)\mathrm{ms}$ (M is the system's total mass, and we use geometric units with $G = c = 1$ throughout).

NSs in field BH–NS binaries may not commonly have $P = \mathcal{O}(\mathrm{ms})$ near merger. However, there are two reasons to think that the opposite may hold for dynamical capture BH–NS mergers occurring in GCs: the pulsar spin period distribution in Galactic GCs peaks in the milliseconds, and millisecond pulsars (MSPs) have longer inferred magnetic dipole spin-down timescales.

Of the 144 currently known pulsars in Galactic GCs, $\sim 83\%$ have periods less than 10 ms, $\sim 55\%$ less than 5 ms, and $\sim 12\%$ have periods less than 2.5 ms [1]. This set includes PSR-J1748-2446ad—the fastest-spinning pulsar known, with $P = 1.396$ ms (Hessels et al. 2006). The theoretical explanation for this skew toward short periods is that GCs favor the formation of low-mass X-ray binaries (LMXB) (Verbunt & Hut 1987), which are thought to spin up the NS to ms periods through mass and angular momentum transfer (Alpar et al. 1982; Radhakrishnan & Srinivasan 1982).

Assuming that pulsar spin-down is predominantly due to magnetic dipole emission, both the magnetic field strength (B) and spin-down timescale (t_{sd}) can be computed from observations of P and its time derivative $\dot{P}$. For B the relation is (Bhattacharya & van den Heuvel 1991)

$$B \sim 1.6 \times 10^8 \text{ G} \left[\frac{P}{2.5 \text{ ms}} \frac{\dot{P}}{10^{-20}} \right]^{1/2},$$

which for known GC MSPs with $\dot{P} > 0$ gives typical values $B \sim 10^8$—10^9G. Observations of X-ray oscillations of accretion-powered MSPs in LMXBs, and pulsar recycling theory imply B in the range 3×10^7—3×10^8G (Lamb & Yu 2005). For t_{sd} the expression is (Zhang & Mészáros 2001)

$$t_{sd} \sim 4 \text{ Gyr} \frac{I}{10^{45}\text{g cm}^2} \left(\frac{B}{3 \times 10^8 \text{ G}} \right)^{-2} \quad (1)$$
$$\left(\frac{P}{2.5 \text{ ms}} \right)^2 \left(\frac{R_{NS}}{10 \text{ km}} \right)^{-6},$$

where the NS moment of inertia is I. Even neglecting the possibility of magnetic field decay, e.g. a pulsar with a magnetic field of 3×10^8G and initial $P = 2.5$ms will take roughly a Hubble time for P to double. Given the long spin-down timescale of MSPs and the results of Lee et al. (2010), which suggest that in GCs there could be 40 BH–NS collisions per Gyr per Milky Way-equivalent galaxy,

[1] www.naic.edu/~pfreire/GCpsr.html

it is at least conceivable that some of these eccentric BH–NS collisions take place with millisecond NSs.

With this motivation, here we focus on eccentric BH–NS mergers (with initial conditions corresponding to a marginally unbound Newtonian orbit) and explore NS spin effects. We show that even moderate spins can significantly impact the outcome, both in terms of the GWs, and amounts of tidally stripped bound and unbound matter. The remainder of the paper is as follows: in Sec. 2 we describe our initial data and numerical methods. In Sec. 3 we present our simulation results and discuss the impact of NS spin on gravitational and EM signatures. We summarize in Sec. 4 and discuss future work.

2. NUMERICAL APPROACH

We perform GR-HD simulations of BHs merging with rotating NSs using the code of East et al. (2012b). The field equations are solved in the generalized-harmonic formulation, using finite differences, while the hydrodynamics are evolved using the same high-resolution shock-capturing techniques as in East et al. (2012a).

To construct initial data, we solve the constraint equations using the code of East et al. (2012c), specifying the free-data as a superposition of a non-spinning BH with an equilibrium, uniformly rotating NS, which we generate using the code of Cook et al. (1994a,b). For the NS EOS, we adopt the HB piece-wise polytrope from Read et al. (2009), and include a thermal component $P_{th} = 0.5\epsilon_{th}\rho$ allowing for shock heating.

Fixing the NS gravitational mass to $1.35M_\odot$, we consider NSs with dimensionless spins $a_{NS} = J/M_{NS}^2 = 0$, 0.1, 0.2, 0.3, 0.4, 0.5, and 0.756, having corresponding compactions (mass-to-equatorial-radius) $C = 0.172$, 0.171, 0.169, 0.166, 0.161, 0.154, and 0.12. The ranges of $T/|W|$ (kinetic-to-gravitational-potential-energy ratio) and P in our spinning NS models are $[0.003, 0.12]$ and $[5.25, 1.00]$ ms. The fastest spinning NS considered has a polar-to-equatorial-radius ratio of $r_{po}/r_{eq} = 0.55$, near the mass-shedding limit of $r_{po}/r_{eq} = 0.543$. We also vary $r_p/M \in [5, 8]$.

We consider systems with $q = 4$. The two COs are initially placed at a separation of $d = 50M$ (~ 500km), with positions and velocities corresponding to a marginally unbound Newtonian orbit labeled by r_p. For this initial study, we only consider cases where the spin is aligned or anti-aligned with the orbital angular momentum (the latter indicated by $a_{NS} < 0$).

The simulations utilize seven levels of adaptive mesh refinement that are dynamically adjusted based on the estimated truncation error of the metric. Most simulations are performed using a base-level resolution with 193^3 points, and finest-level resolution with approximately 75 (130) points covering the (non-spinning) NS (BH) diameter, respectively. For $r_p/M = 6$, $a_{NS} = 0.756$ we also perform simulations at $2/3$ and $4/3\times$ the resolution, to establish convergence and estimate truncation error. In Fig. 1 we demonstrate the convergence in the GW emission.

3. RESULTS AND DISCUSSION

3.1. Simple estimates

During eccentric encounters between NSs and BHs, for NS tidal disruption to form a substantial disk and un-
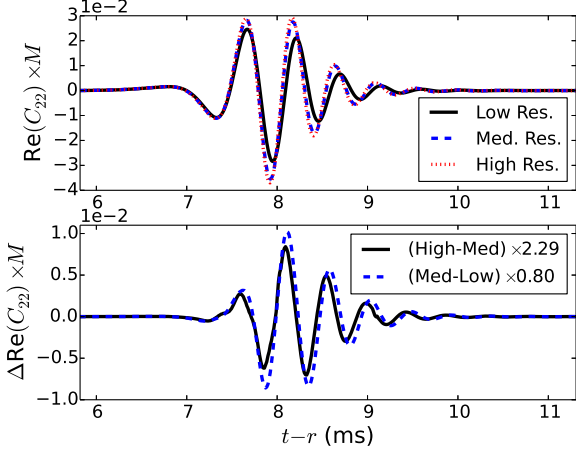
FIG. 1.— Convergence of the GW emission for the $r_p/M = 6$, $a_{\mathrm{NS}} = 0.756$ case. The top panel shows the real part of the $\ell = m = 2$ mode of the Newman–Penrose scalar Ψ_4 at three resolutions, and the bottom panel the differences in this quantity with resolution, scaled assuming second-order convergence.

bind a non-negligible amount of matter, it must occur outside the ISO radius ($r_{\mathrm{ISO}} = 4M_{\mathrm{BH}}$ for a marginally unbound test particle about a non-spinning BH). In addition to shifting the effective ISO, spin makes the NS less self-bound, and thus alters the tidal disruption radius. Equating the sum of the tidal and centrifugal accelerations to the gravitational acceleration on the NS surface yields

$$\frac{r_t}{M_{\mathrm{BH}}} \sim q^{-2/3} C^{-1} \left(\frac{1}{1 - (a_{\mathrm{NS}}/a_{\mathrm{ms}})^2} \right)^{1/3}, \qquad (2)$$

where we replaced the NS angular frequency with $\Omega = J/I = a_{\mathrm{NS}} M_{\mathrm{NS}}^2 / I$, and let $I = 2f M_{\mathrm{NS}} R_{\mathrm{NS}}^2 / 5$, with f an order-unity constant that depends on the NS structure. Here, $a_{\mathrm{ms}} = (4f^2/25C)^{1/2} \simeq 0.8(f/0.7)(C/0.12)^{-1/2}$ is the mass-shedding limit spin parameter. Equation (2) shows that the closer a_{NS} is to a_{ms}, the larger the tidal disruption radius. It also suggests that for sufficiently fast rotators, the tidal disruption radius can be outside the ISO even for large q, something which is not true for non-spinning NSs unless the BH has near-extremal spin. Additionally, as the prograde NS spin increases, the effective ISO decreases. Therefore, we expect more massive disks and more unbound material following tidal disruption outside the ISO with increasing a_{NS}.

3.2. Dynamics and Gravitational Waves

For the cases considered here, those with $r_p \leq 6.5$ merge on the initial encounter, while those with $r_p \geq 7.5$ go back out on an elliptic orbit after fly-by. Figure 2 plots the dominant contribution to the GW signal for $r_p/M = 6$, 7, and 8; see also Table 1. Near the critical r_p — below (above) where a merger (fly-by) occurs — there are large differences in the dynamics that have a noticeable impact on the GW signal and tidally stripped matter. This is evident here with the $r_p/M = 7$ case, where there is either partial tidal disruption followed by a merger on a second encounter (for $a_{\mathrm{NS}} = 0.4$ and 0.5), or complete tidal disruption/merger on the first encounter (for the other spins). This is illustrated in Fig. 3 for
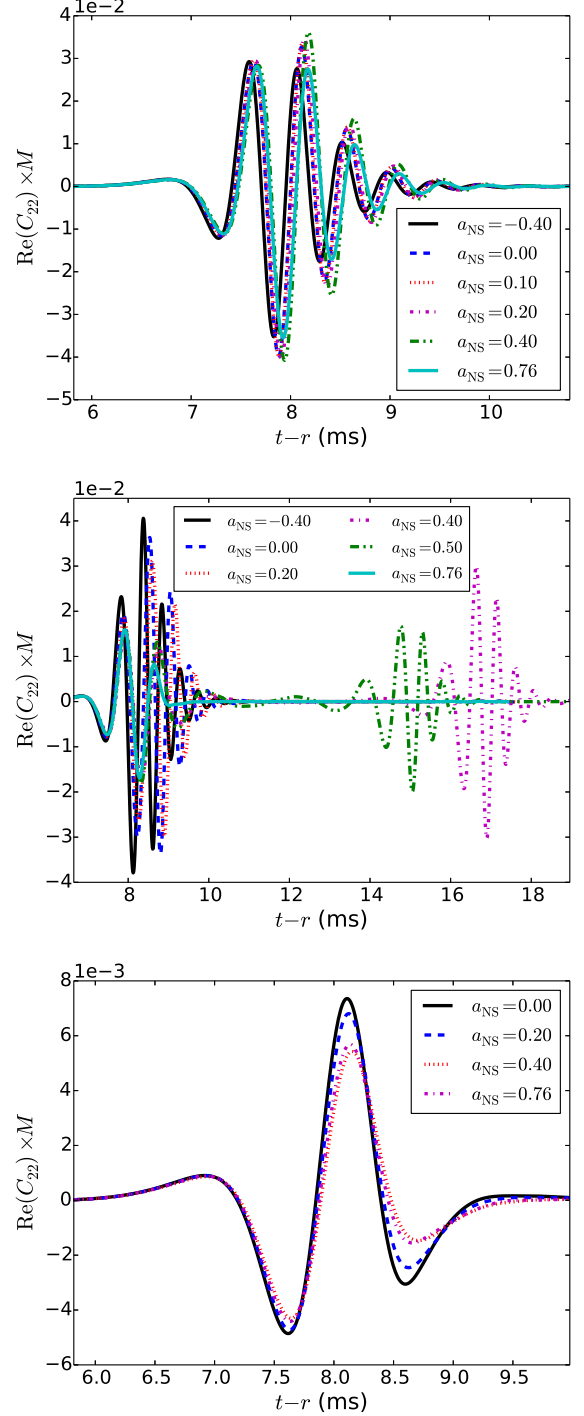

FIG. 2.— Plots of the real part of the $l = m = 2$ mode of the scalar Ψ_4. The top and middle panels show GWs from simulations with $r_p/M = 6$ and 7, respectively. The bottom panel plots the GWs for $r_p/M = 8$ fly-by cases.

$a_{\mathrm{NS}} = 0.2, 0.5$, as well as the bottom-right panel of Fig. 4 where it can be seen that the NS for $a_{\mathrm{NS}} = 0.4$ (0.5) loses $\sim 10\%$ ($\sim 20\%$) of its mass in the initial encounter.

Though it is difficult to disentangle the nonlinear dynamics occurring here, we suggest the following explanation for this non-monotonic behavior as a function of a_{NS} for $r_p/M = 7$. The $a_{\mathrm{NS}} = 0.756$ NS is the least

bound and for this case complete tidal disruption occurs on the initial encounter. As the NS is tidally stretched, GW emission effectively shuts off (middle panel Fig. 2), and matter begins to accrete onto the BH (bottom panel of Fig. 4). For the next two lower spins, the material is more tightly bound, and only partial disruption occurs, with some of the material promptly accreting onto the BH. However, as the NS spin decreases, the effective ISO radius increases, and for $a_{\rm NS} \lesssim 0.3$ the core of the NS crosses the ISO, resulting in immediate merger. The $a_{\rm NS} = 0.4$ and 0.5 cases lose enough orbital energy and angular momentum during the first encounter that they merge on the second.

Note that the simple estimate of Equation (2) implies that since at $r_p/M = 7$ the $a_{\rm NS} = 0.756$ case is completely disrupted, while some of the lower spin cases are partially disrupted, $r_p/M = 8, a_{\rm NS} = 0.756$ should also be disrupted, given how close this spin is to the break up value. That this does *not* happen shows that this crude estimate significantly underestimates the self-binding of high spin stars.

3.3. *Post-merger Matter Distribution*

In Table 1 we list the amount of bound and unbound mass exterior to the BH shortly following merger. For $r_p/M = 5, 6$ the bound mass is only a weak function of $a_{\rm NS}$, with the notable exception of $a_{\rm NS} = 0.756, r_p/M = 6$. By contrast, near the critical impact parameter ($r_p/M = 7$) there is over an order of magnitude variation in bound material as a function of NS spin.

The amount of bound rest-mass that forms a BH accretion disk is 0.01–$0.15 M_\odot$ in our set. If these disks power sGRBs on timescales of ~ 0.2s, the accretion rates will be ~ 0.05–$0.75 M_\odot$ s^{-1}, i.e., consistent with magneto-hydrodynamic BH–NS studies (Paschalidis et al. 2014). Assuming a 1% conversion efficiency of accretion power to jet luminosity, these accretion rates imply luminosities of 10^{51}–10^{52}erg s^{-1}—consistent with characteristic sGRB luminosities.

The top two panels in Fig. 4 show plots of the asymptotic velocity distribution of the unbound matter for $r_p/M = 6, 7$. As anticipated (see Sec. (3.1)), the general trend is that increasing $a_{\rm NS}$ increases both the amount and average asymptotic velocity of unbound material. This is also seen in Table 1 where we list these quantities for all cases. The bottom-left panel of Fig. 4 also demonstrates that including spin increases the amount of unbound material by an order of magnitude or more for the cases considered.

The increase in total rest-mass $M_{0,{\rm u}}$ and velocity v of the unbound material with increasing $a_{\rm NS}$ can strongly impact potential kilonovae signatures from such mergers. These arise when neutron-rich ejecta produce heavy elements through the r-process than then undergo fission, emitting photons (Li & Paczynski 1998; Kulkarni 2005). Recently Barnes & Kasen (2013) have shown that the opacities in r-process ejecta will likely be dominated by lanthanides, giving rise times of

$$t_{\rm peak} \approx 0.25 (M_{0,{\rm u}}/10^{-2}\ M_\odot)^{1/2} (v/0.3c)^{-1/2}\ {\rm d}$$

with peak luminosities of

$$L \approx 2 \times 10^{41} \left(\frac{M_{0,{\rm u}}}{10^{-2}\ M_\odot} \right)^{1/2} \left(\frac{v}{0.3c} \right)^{1/2}\ {\rm erg\ s}^{-1} \quad (3)$$

for typical values found here. In some cases, opacities an order of magnitude lower than those used above may be justified (Metzger et al. 2015). Using Eq. (3) we estimate the luminosity from potential kilonovae in Table 1. Apart from the fact that NS spin can make the difference in whether there will be a kilonova at all for $r_p/M = 5$, for $r_p/M = 6$ and $r_p/M = 7$ spin affects L by an order of magnitude in our set. For $r_p/M = 6$ even a moderate $a_{\rm NS} = 0.1$ increases L by a factor of 4 compared to $a_{\rm NS} = 0$. Barnes & Kasen (2013) predict that a kilonova luminosity of $\sim 10^{41}$erg s^{-1} corresponds to an r-band magnitude of 23.5 mag at 200 Mpc (near the edge of the aLIGO volume), above the planned LSST survey sensitivity of 24.5 mag. Thus, differences in luminosity by factors of a few could be discernible.

Ejecta will also sweep the interstellar medium (ISM) producing radio waves. These will peak on timescales of weeks with brightness (Nakar & Piran 2011)

$$F(\nu_{\rm obs}) \approx 0.6 (E_{\rm kin}/10^{51}\ {\rm erg})(n_0/0.1\ {\rm cm}^{-3})^{7/8} \quad (4)$$
$$(v/0.3c)^{11/4} (\nu_{\rm obs}/{\rm GHz})^{-3/4} (d/100\ {\rm Mpc})^{-2}\ {\rm mJy}$$

for an observation frequency $\nu_{\rm obs}$ at a distance d, and using $n_0 \sim 0.1$ cm^{-3} as the density for GC cores (Rosswog et al. 2013). Estimating the kinetic energy and the mass-averaged velocity in the ejecta, we show $F(\nu_{\rm obs})$ via Eq. (4) in Table 1. For $r_p/M = 6$ ($r_p/M = 7$) $F(\nu_{\rm obs})$ varies by 3 (2) orders of magnitude over our set of spins.

Finally, it has been suggested that ejecta from mergers involving NSs may make a non-negligible contribution to the overall abundance of r-process elements (Lattimer & Schramm 1974; Rosswog et al. 1998). In particular, dynamical-capture binaries, which can form and merge on shorter timescales, may be favored over field binaries in explaining abundances in carbon-enhanced metal-poor stars (Ramirez-Ruiz et al. 2014). The average galactic production of these elements is estimated to be $\sim 10^{-6} M_\odot$ yr^{-1} (Qian 2000). Making the limiting assumption that all r-process material comes from extreme BH-NS mergers cases like the $r_p = 7$, $a_{\rm NS} = 0.76$ with $M_{0,{\rm u}} \approx 0.3 M_\odot$ caps these extreme events at 3×10^{-6} yr^{-1} per galaxy (similar to predicted rates for primordial BH–NS mergers (Abadie et al. 2010)).

4. CONCLUSIONS

We have demonstrated using GR-HD simulations of dynamical capture BH–NS mergers that even moderate values of NS spin can significantly increase the mean velocity and amount of unbound material (to as much as $0.3 M_\odot$ for extreme spins). This could lead to significantly brighter transients, including kilonovae a factor of a few brighter, and radio wave emission from interaction with the ISM an order of magnitude or more brighter. For comparison, simulations of quasicircular BH–NS mergers with nonspinning NSs typically find ejecta velocities ~ 0.2–$0.3c$, comparable, though somewhat smaller than found here, but only find similar amounts of ejected material for cases with smaller mass-ratios and/or high BH spin (Kyutoku et al. 2015). We also find that the NS spin can alter the amount of bound matter that, following tidal disruption, remains to form an accretion disk that may power a sGRB. Depending
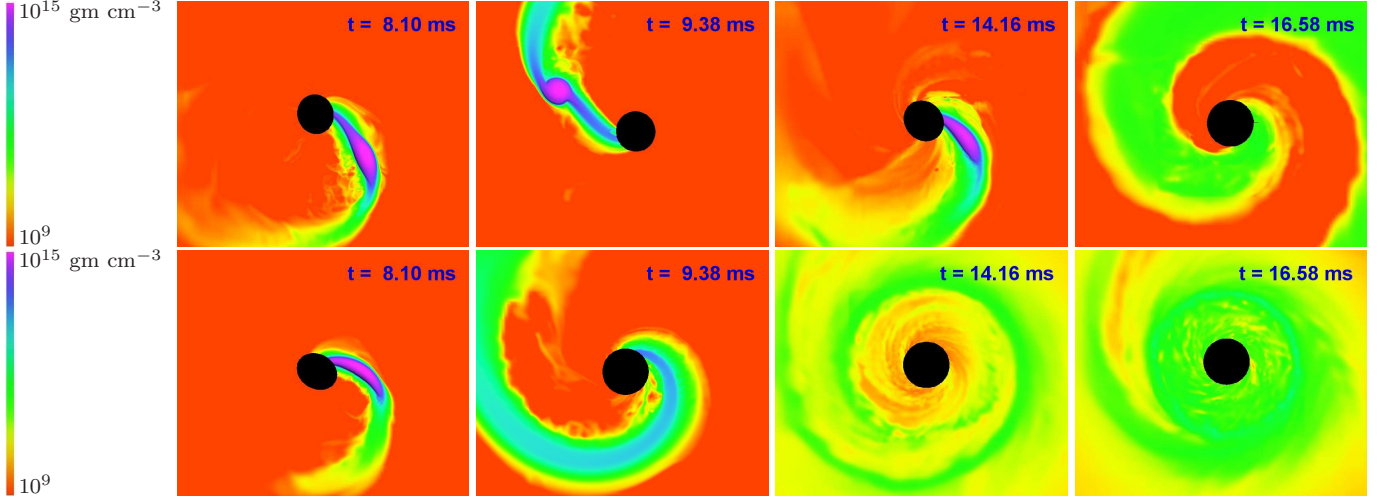
FIG. 3.— Equatorial density snapshots. Top row ($r_p/M = 7$, $a_{NS} = 0.5$) from left to right: the NS survives the first encounter (first and second panels), it is completely tidally disrupted during the second encounter (third panel), the bulk of the matter outside the BH is unbound (fourth panel). Bottom row ($r_p/M = 7$, $a_{NS} = 0.2$) from left to right: the NS is tidally disrupted during the first encounter (first panel), a tidal tail forms ejecting some matter to infinity (second panel), an accretion disk develops outside the BH (third and fourth panels). The scale can be inferred from the size of the BH ($R_{BH} \sim 16$ km).
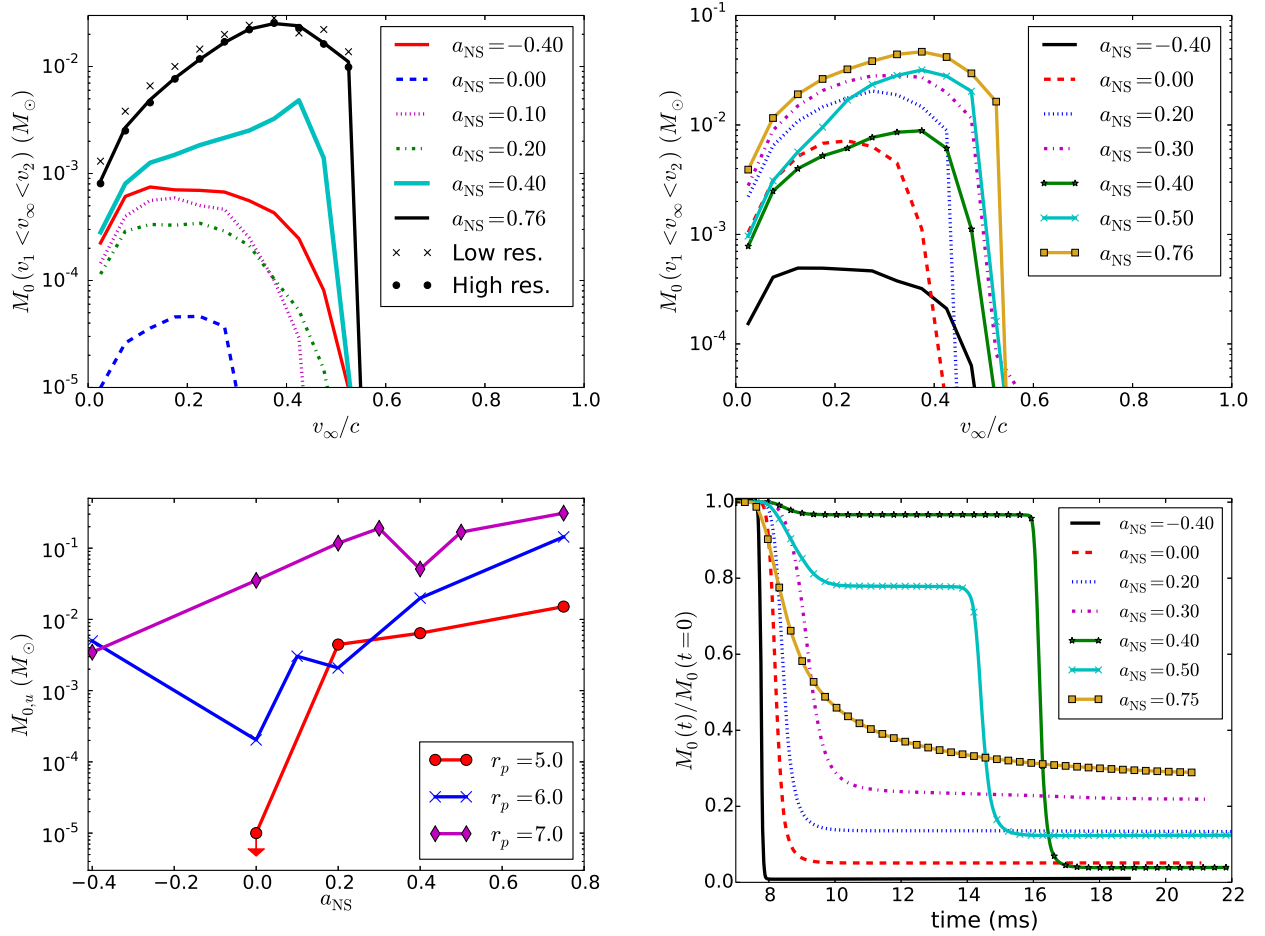

FIG. 4.— Top: distribution of the asymptotic velocity of unbound rest-mass, binned in increments of $0.05c$, and computed ≈ 10 ms post-merger for $r_p/M = 6$ (left) and $r_p/M = 7$ (right) and various spins. Bottom: total unbound mass as a function of NS spin (left) and rest-mass outside the BH versus time for $r_p/M = 7$ and various spins (right). Note that for the lowest point in the bottom-left panel, no unbound matter was found in the simulation (indicated by an arrow).

r_p	$a_{\rm NS}$	$\frac{J_{\rm ADM}}{M^2}$[a]	$\frac{E_{\rm GW}}{M} \times 100$[b]	$\frac{J_{\rm GW}}{M^2} \times 100$[c]	$M_{0,b}$[d]	$M_{0,u}$[e]	$<v_\infty>$[f]	$E_{\rm kin,51}$[g]	L_{41}[h]	F_ν[i]	$a_{\rm BH}$[j]
5.0	0.00	0.52	0.71	4.33	1.11	0.00	0.0	0.0	0.0	0.0	0.50
5.0	0.20	0.52	0.73	4.51	0.96	0.44	0.20	0.09	1.1	0.02	0.51
5.0	0.40	0.53	0.81	4.95	0.94	0.64	0.19	0.3	1.3	0.05	0.51
5.0	0.75	0.55	0.81	4.97	1.12	1.51	0.42	3.0	2.9	4.5	0.51
6.0	-0.40	0.55	0.92	5.66	1.01	0.50	0.22	0.3	1.2	0.08	0.51
6.0	0.00	0.56	1.13	6.86	1.15	0.02	0.18	0.007	0.2	0.001	0.52
6.0	0.10	0.57	1.16	7.47	1.07	0.30	0.19	0.1	0.9	0.02	0.53
6.0	0.20	0.57	1.21	7.30	1.10	0.21	0.20	0.1	0.7	0.02	0.54
6.0	0.40	0.58	1.31	8.03	0.91	1.99	0.32	2.3	2.9	1.6	0.53
6.0	0.75	0.60	1.04(1.23)[k]	6.85(7.92)	2.40(2.23)	14.39(14.01)	0.346(0.350)	19.9	8.2	17.9	0.491 (0.492)
6.5	0.40	0.60	1.51	9.91	4.39	9.08	0.28	8.0	5.8	3.8	0.50
7.0	-0.40	0.63	1.51	9.38	1.17	0.35	0.23	0.2	1.0	0.06	0.53
7.0	0.00	0.61	1.72	11.65	4.31	3.53	0.21	1.7	3.1	0.4	0.51
7.0	0.20	0.62	1.68	12.13	8.95	11.73	0.26	8.6	6.3	3.4	0.47
7.0	0.30	0.62	1.52	12.75	15.34	18.98	0.28	17.3	8.5	8.8	0.40
7.0	0.40	0.63	2.12	18.27	0.94	5.10	0.28	4.6	4.4	2.3	0.45
7.0	0.50	0.63	1.65	15.39	2.06	16.80	0.33	20.4	8.6	16.1	0.50
7.0	0.75	0.64	0.70	6.95	12.43	30.98	0.32	36.6	11.4	25.3	0.37

TABLE 1
SUMMARY OF SIMULATIONS FOLLOWED THROUGH MERGER.

For $r_p/M \geq 7.5$ only the first fly-by encounter was modeled, hence no information related to disrupted material is available. The energy and angular momentum emitted in GWs for these cases drops with increasing r_p after the first encounter, as expected. To within the estimated 20% truncation error inferred from the $r_p = 6$ case resolution study, we see no variation with spin. However, even a small variation in the energy emission at fly-by could result in a significant change in the time to the subsequent close encounter in a highly eccentric binary. Thus, higher resolution studies would be needed to ascertain the effect of spin on the GW signal for $r_p/M \geq 7.5$.

[a] ADM angular momentum.
[b] Total energy emitted in GWs through the $r = 100M$ surface.
[c] Total angular momentum emitted in GWs.
[d] Bound rest mass outside the BH ~ 10 ms post-merger in percent of $M_\odot$.
[e] Unbound rest mass in percent of $M_\odot$.
[f] Rest-mass averaged asymptotic velocity of unbound material.
[g] Kinetic energy of ejecta in units of 10^{51} erg.
[h] Kilonovae bolometric luminosity in units of 10^{41} erg s^{-1} using Eq. (3).
[i] Specific brightness from ejecta interaction with ISM in units of mJy using Eq. (4).
[j] Remnant BH dimensionless spin.
[k] Values in parentheses are Richardson extrapolated values using all three resolutions.

on the impact parameter and NS spin, these mergers can produce accretion disks of up to a tenth of a solar mass.

We find that near the critical impact parameter the NS spin influences the orbital dynamics to a sufficient extent to affect whether a merger or fly-by occurs, with a corresponding large effect on the GW emission. At a first glance this variability might seem exceedingly rare, requiring a finely tuned impact parameter. However, since the primary source of this sensitivity to binary parameters arises because the pericenter gets close to the region of unstable orbits, which exists for all eccentricities, not merely the initially hyperbolic case considered here, one can speculate that the last few encounters for any case where non-negligible orbital eccentricity remains will be subject to this sensitivity. Likewise, the variability associated with EM counterparts could also be present for a larger range of initial impact parameters. Future simulations of multi-burst events will be needed to address this speculation. At the other end of the spectrum, some fraction of dynamical-capture binaries that form at larger initial separations will circularize prior to merger due to GW emission; the results found here thus also motivate the study of quasicircular mergers involving millisecond NSs.

We have shown it is important to include spin to understand the full range of possible EM and GW outcomes in eccentric mergers. However, whether it will be possible to perform parameter estimation from a putative multi-messenger event is a different question. Certainly in a single burst event the degeneracies will be too strong to, for example, identify NS spin as the sole reason for an unusually bright counterpart. Multi-burst events can in principle lift much of the degeneracy, as information in the timing of the bursts could significantly narrow the parameters of the progenitor binary. The range of viable NS EOSs, NS spin directions, and BH spins needs to be simulated, both to determine how these parameters affect the observable outcomes, and how they add to or lift degeneracies. GW detection rates and parameter estimation also needs to be investigated within a realistic data analysis framework including detector noise. All of these problems we leave for future studies. We also plan to study the effect of spin in dynamical-capture NS–NS mergers.

REFERENCES

Abadie, J. et al. 2010, Classical and Quantum Gravity, 27, 173001, 1003.2480

Abramovici et al., A. 1992, Science, 256, 325

Alpar, M. A., Cheng, A. F., Ruderman, M. A., & Shaham, J. 1982, Nature, 300, 728

Barnes, J., & Kasen, D. 2013, ApJ, 775, 18, 1303.5787

Bernuzzi, S., Dietrich, T., Tichy, W., & Bruegmann, B. 2014, Phys.Rev., D89, 104021, 1311.4443

Bhattacharya, D., & van den Heuvel, E. 1991, Physics Reports, 203, 1

Chawla, S., Anderson, M., Besselman, M., Lehner, L., Liebling, S. L., Motl, P. M., & Neilsen, D. 2010, Physical Review Letters, 105, 111101

Cook, G. B., Shapiro, S. L., & Teukolsky, S. A. 1994a, ApJ, 424, 823

——. 1994b, ApJ, 422, 227

East, W. E., McWilliams, S. T., Levin, J., & Pretorius, F. 2013, Phys. Rev. D, 87, 043004, 1212.0837

East, W. E., Pretorius, F., & Stephens, B. C. 2012a, Phys. Rev. D, 85, 124009

——. 2012b, Phys. Rev. D, 85, 124010

East, W. E., Ramazanoglu, F. M., & Pretorius, F. 2012c, Phys.Rev., D86, 104053, 1208.3473

Etienne, Z. B., Paschalidis, V., & Shapiro, S. L. 2012, Phys.Rev., D86, 084026

Foucart, F., Deaton, M. B., Duez, M. D., O'Connor, E., Ott, C. D., et al. 2014, Phys.Rev., D90, 024026

Hansen, B. M., & Lyutikov, M. 2001, Mon.Not.Roy.Astron.Soc., 322, 695, astro-ph/0003218

Hessels, J. W., Ransom, S. M., Stairs, I. H., Freire, P. C. C., Kaspi, V. M., et al. 2006, Science, 311, 1901, astro-ph/0601337

Kocsis, B., & Levin, J. 2012, Phys. Rev. D, 85, 123005, 1109.4170

Kulkarni, S. R. 2005, ArXiv Astrophysics e-prints, arXiv:astro-ph/0510256

Kyutoku, K., Ioka, K., Okawa, H., Shibata, M., & Taniguchi, K. 2015, ArXiv e-prints, 1502.05402

Kyutoku, K., Ioka, K., & Shibata, M. 2013, Phys.Rev., D88, 041503

Lamb, F., & Yu, W. 2005, in Astronomical Society of the Pacific Conference Series, Vol. 328, Binary Radio Pulsars, ed. F. A. Rasio & I. H. Stairs, 299, astro-ph/0408459

Lattimer, J. M., & Schramm, D. N. 1974, ApJ, 192, L145

Lee, W. H., Ramirez-Ruiz, E., & van de Ven, G. 2010, ApJ, 720, 953, 0909.2884

Li, L.-X., & Paczynski, B. 1998, Astrophys.J., 507, L59, astro-ph/9807272

LSST Dark Energy Science Collaboration. 2012, ArXiv e-prints, 1211.0310

McWilliams, S. T., & Levin, J. 2011, ApJ, 742, 90, 1101.1969

Meszaros, P. 2006, Rept.Prog.Phys., 69, 2259

Metzger, B. D., Bauswein, A., Goriely, S., & Kasen, D. 2015, MNRAS, 446, 1115, 1409.0544

Metzger, B. D., & Berger, E. 2012, ApJ, 746, 48, 1108.6056

Nakar, E., & Piran, T. 2011, Nature, 478, 82, 1102.1020

Paschalidis, V., Etienne, Z. B., & Shapiro, S. L. 2013, Phys.Rev., D88, 021504

Paschalidis, V., Ruiz, M., & Shapiro, S. L. 2014, 1410.7392

Qian, Y.-Z. 2000, ApJ, 534, L67, astro-ph/0003242

Radhakrishnan, V., & Srinivasan, G. 1982, Current Science, 51, 1096

Ramirez-Ruiz, E., Trenti, M., Roberts, L. F., Lee, W. H., & Saladino-Rosas, M. I. 2014, ArXiv e-prints, 1410.3467

Rau, A. e. a. 2009, PASP, 121, 1334, 0906.5355

Read, J. S., Markakis, C., Shibata, M., Uryū, K., Creighton, J. D. E., & Friedman, J. L. 2009, Phys. Rev. D, 79, 124033, 0901.3258

Rosswog, S., Piran, T., & Nakar, E. 2013, MNRAS, 430, 2585, 1204.6240

Rosswog, S., Thielemann, F. K., Davies, M. B., Benz, W., & Piran, T. 1998, in Nuclear Astrophysics, ed. W. Hillebrandt & E. Muller, 103, arXiv:astro-ph/9804332

Samsing, J., MacLeod, M., & Ramirez-Ruiz, E. 2014, Astrophys.J., 784, 71, 1308.2964

Stephens, B. C., East, W. E., & Pretorius, F. 2011, ApJ, 737, L5, 1105.3175

Tai, K. S., McWilliams, S. T., & Pretorius, F. 2014, Phys.Rev., D90, 103001, 1403.7754

Tanaka, M., Hotokezaka, K., Kyutoku, K., Wanajo, S., Kiuchi, K., et al. 2014, Astrophys.J., 780, 31

Tichy, W. 2011, Phys.Rev., D84, 024041, 1107.1440

Verbunt, F., & Hut, P. 1987, in IAU Symposium, Vol. 125, The Origin and Evolution of Neutron Stars, ed. D. J. Helfand & J.-H. Huang, 187

Zhang, B., & Mészáros, P. 2001, ApJ, 552, L35, astro-ph/0011133